

2012

# A Calibration Procedure for Measuring the Thermal Conductivity of Molten Salts at Elevated Temperatures

Benjamin Rosenzweig  
*Lehigh University*

Follow this and additional works at: <http://preserve.lehigh.edu/etd>

---

## Recommended Citation

Rosenzweig, Benjamin, "A Calibration Procedure for Measuring the Thermal Conductivity of Molten Salts at Elevated Temperatures" (2012). *Theses and Dissertations*. Paper 1074.

This Thesis is brought to you for free and open access by Lehigh Preserve. It has been accepted for inclusion in Theses and Dissertations by an authorized administrator of Lehigh Preserve. For more information, please contact [preserve@lehigh.edu](mailto:preserve@lehigh.edu).

# A Calibration Procedure for Measuring the Thermal Conductivity of Molten Salts at Elevated Temperatures

by

Benjamin Rosenzweig

A Thesis

Presented to the Graduate and Research Committee

of Lehigh University

in Candidacy for the Degree of

Master of Science

in

Mechanical Engineering and Mechanics

Lehigh University

May 2012

© 2012  
Benjamin M. Rosenzweig

All Rights Reserved

This thesis is accepted and approved in partial fulfillment of the requirements for the Master of Science.

---

Date

---

Dr. Alparslan Oztekin, Thesis Advisor

---

Dr. Sudhakar Neti, Thesis Co-Advisor

---

Dr. D. Gary Harlow, Chairperson of Department

## **Acknowledgments**

I would like to express my greatest appreciation to my thesis advisors, Professors Alparslan Oztekin and Sudhakar Neti. They have provided the mentorship necessary to aid me in completing my research. I would also like to thank Dynalene for providing the facilities and staff to help complete my research experiments. Finally, I would like to thank my family and friends who have supported and encouraged me throughout the completion of my educational career.

# Table of Contents

<b>Acknowledgments</b> .....	<b>iv</b>
<b>List of Tables</b> .....	<b>vii</b>
<b>List of Figures</b> .....	<b>viii</b>
<b>List of Nomenclature</b> .....	<b>ix</b>
<b>Abstract</b> .....	<b>1</b>
<b>Chapter 1: Introduction</b> .....	<b>2</b>
<b>1.1 Motivation</b> .....	<b>2</b>
<b>1.2 Literature Review</b> .....	<b>3</b>
1.2.1 Measuring the Thermal Conductivity of Solids.....	3
1.2.2 Measuring the Thermal Conductivity of Liquids .....	5
<b>Chapter 2: Measuring Thermal Conductivity</b> .....	<b>9</b>
<b>2.1 Definition of Thermal Conductivity</b> .....	<b>9</b>
2.2 Steady State Thermal Conductivity Measurement .....	9
2.3 Transient Thermal Conductivity Measurement .....	10
<b>2.4 Choice of Measurement Technique for Current Research</b> .....	<b>13</b>
<b>Chapter 3: Mathematical Model and Solutions</b> .....	<b>15</b>
<b>3.1 Theoretical Solution</b> .....	<b>15</b>
3.1.1 Theoretical Solution Sensitivity Analysis .....	20
<b>3.2 Numerical Simulation</b> .....	<b>23</b>
<b>3.3 Comparison of Numerical and Series Solutions</b> .....	<b>24</b>

<b>Chapter 4: Experimental Analysis.....</b>	<b>26</b>
<b>4.1 Calibration Experiment Procedure .....</b>	<b>26</b>
<b>4.2 Calibration Experiments .....</b>	<b>27</b>
4.2.1 Water at 23 Degrees Celsius.....	27
4.2.2 Propylene Glycol at 24 Degrees Celsius.....	30
4.2.3 Propylene Glycol at 60 Degrees Celsius.....	32
4.2.4 Propylene Glycol at 80 Degrees Celsius.....	34
4.2.5 Propylene Glycol at 100 Degrees Celsius.....	36
<b>4.4 Summary of Calibration Experiments .....</b>	<b>38</b>
<b>Chapter 5: Summary and Conclusions.....</b>	<b>40</b>
<b>References .....</b>	<b>42</b>
<b>Appendix A – Numerical Solution of Governing PDE.....</b>	<b>44</b>
<b>Appendix B – Curve Fitting and Data Analysis .....</b>	<b>45</b>
<b>Vita.....</b>	<b>48</b>

## List of Tables

Table 1: Property Table for Water at 23 C .....	27
Table 2: Summary of Results for Water at 23 C .....	30
Table 3: Property Table for Propylene Glycol at 24 C .....	30
Table 4: Summary of Results for Propylene Glycol at 100 C .....	32
Table 5: Property Table for Propylene Glycol at 60 C .....	32
Table 6: Summary of Results for Propylene Glycol at 60 C .....	34
Table 7: Property Table for Propylene Glycol at 80 C .....	34
Table 8: Summary of Results for Propylene Glycol at 100 C .....	36
Table 9: Property Table for Propylene Glycol at 100 C .....	36
Table 10: Summary of Results for Propylene Glycol at 100 C .....	38



## List of Figures

Figure 1: Concentric Cylinder Apparatus.....	4
Figure 2: Comparison of Thermal Conductivity Data for Solid Potassium Nitrate .....	5
Figure 3: Hot Wire Assembly, 1 – Terminal, 2 – Cu Packaging, 3 – Teflon Packing, 4 – Pressure Vessel, 5 – Insulated Pt Wire, 6 – Sus Rod, 7 – ABS Disk, 8 – Grand Retaining Ring, 9 – Insulated Cu Rod.....	7
Figure 4: Schematic of cross-section of divided-bar apparatus.....	10
Figure 5: Laser Flash Apparatus Design .....	13
Figure 6: Model Geometry .....	15
Figure 7: Theoretical Sensitivity Analysis For "Long" Times .....	21
Figure 8: Theoretical Sensitivity Analysis For "Short" Times.....	22
Figure 9: Series Solution Plotted with Numerical Solution .....	25
Figure 10: Temperature Response of Water at 23 C .....	28
Figure 11: Slope Comparison of Experimental Data to Series Solution for Water at 23 C .....	29
Figure 12: Temperature Response Slope of Propylene Glycol at 24 C.....	31
Figure 13: Temperature Response Slope of Propylene Glycol at 60 C.....	33
Figure 14: Temperature Response Slope of Propylene Glycol at 80 C.....	35
Figure 15: Temperature Response Slope of Propylene Glycol at 100 C.....	37

## List of Nomenclature

$k_s$	Thermal conductivity of sample for Divided Bar Method
$k_g$	Thermal conductivity of reference material for Divided Bar Method
$d$	Thickness of sample for Divided Bar Method
$l$	Total thickness of reference material for Divided Bar Method
$R$	Resistance of bar for Divided Bar Method
$\rho$	Density
$c_p$	Constant pressure specific heat capacity
$T$	Temperature
$t$	Time
$k$	Thermal conductivity
$Q$	Heat generation per unit surface area
$r_0$	Platinum wire radius
$q$	Heat flux per unit length of wire
$\alpha$	Thermal diffusivity of test material for transient line source method
$\gamma$	Euler's constant
$\tau$	Non-dimensional time
$\theta$	Non-dimensional temperature
$\theta_0$	Non-dimensional temperature at wire interface
$K_0$	Modified Bessel function of zero order
$K_1$	Modified Bessel function of first order
$T_0$	Temperature at wire interface

## **Abstract**

The work presented here describes a method for calibrating a recently designed device that will measure the thermal conductivity of liquids at elevated temperatures. Molten salts are addressed in this research, as they are becoming a highly researched topic as phase change materials and heat transfer fluids in relation to thermal energy storage in the solar industry. Because there is no conclusive experiment in which the thermal conductivity of molten salts has been measured, a device has been designed and calibrated for this specific task. The function introduced herein is an asymptotic solution to the transient diffusion equation and is used to curve fit the experimentally determined temperature versus time data to calculate the thermal conductivity of the test liquids at various elevated temperatures. Experiments were conducted on water and propylene glycol as part of the calibration procedure. For water at 23 C, the measured thermal conductivity values were within 3 % of the literature value for all experimental trials. For propylene glycol over a temperature range from 24 C to 100 C, percent errors of up to 19 % were found. The high error found in the propylene glycol experiments is due to the poor temperature control of the available test furnace. In order to reduce error a furnace with a higher degree of temperature control must be used in order to achieve equilibrium within in the test liquid.

# Chapter 1: Introduction

## 1.1 Motivation

As the energy crisis becomes a more serious global issue, new technology for renewable energy and energy storage is being pursued. Methods of harvesting solar energy have become popular all over the world; the problem is that there is no highly efficient method to store the energy that is collected. The promise of storing thermal energy in phase change materials and transferring this energy in high efficiency heat transfer fluids is a driving force behind the current research in advanced thermal energy storage techniques.

Taking advantage of the latent heat of phase change properties in any phase change material can increase the efficiency of an energy storage system significantly. Latent heat yields a much more efficient means of storage than sensible heat, which has been a more popular method of energy storage in the past. The most common phase change materials are water, metals, salts, and salt mixtures. The properties of water and metals have been well documented for years. Current research shows that salts and salt mixtures are ideal candidates for phase change materials to be used in thermal energy storage applications. The issue here is that the properties of these salts and salt mixtures are not well known. In order to calculate and simulate the performance of these materials, the thermal conductivity must be determined. Therefore, the motivation for this research is to reliably measure the thermal conductivity of select molten salts in order to be able to further advance the current research in thermal energy storage and heat transfer.

## **1.2 Literature Review**

### **1.2.1 Measuring the Thermal Conductivity of Solids**

Currently, research in the measurement of the thermal conductivity of solids is being widely pursued. Measuring the thermal conductivity of solids at both high and low temperatures is important, especially when the solids being considered may be used as phase change materials for energy storage purposes. It is crucial to have accurate thermal conductivity data for the solids in questions at the range of temperature that will be encountered during the solid's use as a storage medium.

Many experimental techniques have been employed to measure the thermal conductivity of solids, specifically solid salts such as nitrates. Bloom, et al [1] used the concentric cylinder apparatus to measure the thermal conductivity of alkali nitrates. White and Davis also did comparable experiments using the concentric cylinder apparatus [2]. Turnbull, on the other hand, used the hot wire method to measure the thermal conductivity of the same alkali nitrates [3]. White concluded in his paper, that the hot wire method used by Turnbull was not accurate due to the electrical conductivity of the salts being tests, therefore yielding inaccurate results.

The concentric cylinder apparatus described above, is displayed below, in Figure 1.

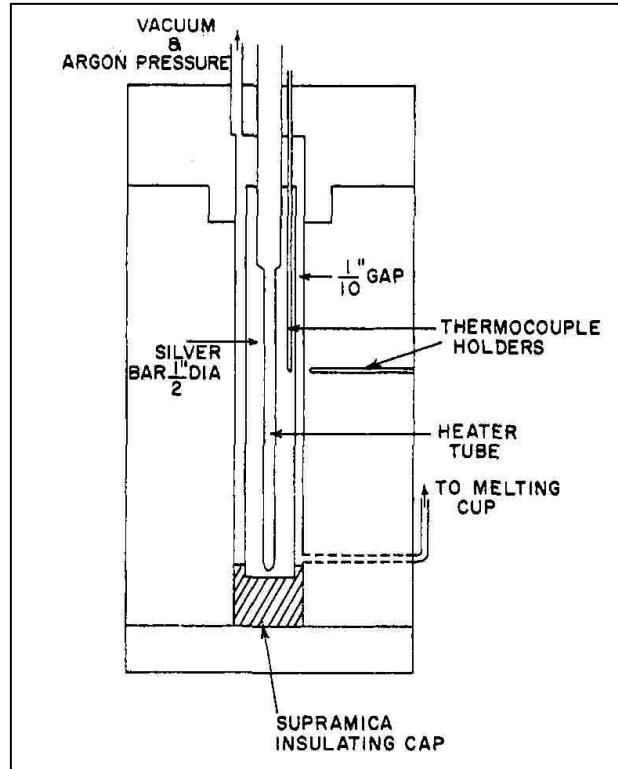


**Figure 1: Concentric Cylinder Apparatus**

This device is used by McDonald and Davis to verify the experiments of Bloom, White, and Turnbull [4]. The results of McDonald and Davis' experiments are compared to Bloom, White, and Turnbull below, and demonstrate how different measurement techniques yield varying results for the same test medium. The variation in results is not only a function of the differing techniques, but it is relative to the uncertainty of each technique as well.

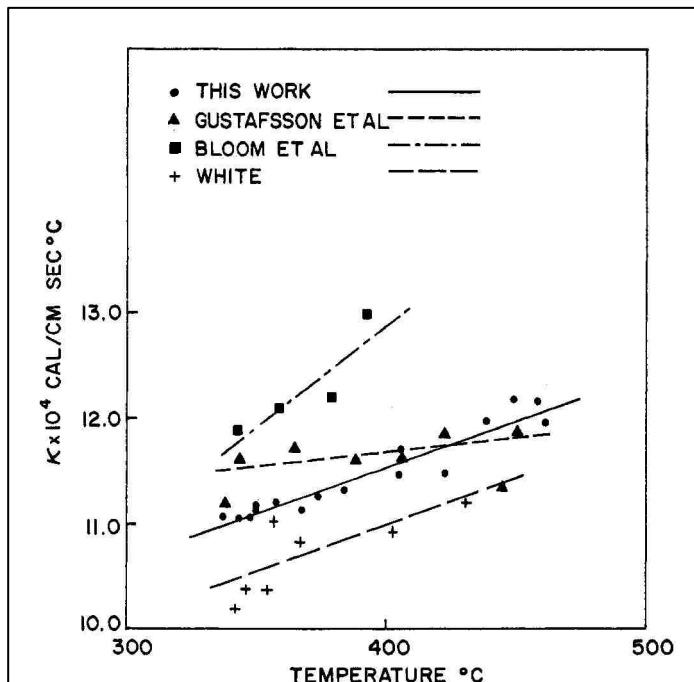


**Figure 2: Comparison of Thermal Conductivity Data for Solid Potassium Nitrate**

As shown in Figure 2, the data for these experiments differ significantly. This is the main reason that further research into more accurate thermal conductivity measurements is necessary.

### 1.2.2 Measuring the Thermal Conductivity of Liquids

Similarly to the thermal conductivity measurements of solids, explained in section 1.2.1, the thermal conductivity measurements of liquids are of equal importance. The measurement of this property for liquids at varying temperatures is of greater importance because it has been historically more difficult to achieve accurate, repeatable, thermal conductivity measurements of liquids, especially at high temperatures. The measurement of the thermal conductivity for any liquid is relatively more difficult to obtain than a

solid, but the thermal conductivity of liquids, near the melting point of the material is more difficult to obtain because environmental control systems need to be used.

The most popular method for measuring the thermal conductivity of liquids is the transient hot wire method. This method is the most widely used because convective heat transfer does not exist in these experiments. By eliminating convective heat transfer; only conduction and radiation need to be addressed. Furthermore, radiation can be neglected at relatively low temperatures, as it is only dominant at higher temperatures [5]. Pittman, Haarman, and Mani have all performed experiments measuring the thermal conductivity of liquids at varying temperatures with high accuracy and repeatability [6, 7, 8]. All of their experimental results compliment each other and prove the accuracy and repeatability of the hot wire method.

Much research has been conducted in improving the hot wire method and correcting any small inaccuracies that might exist. It has been determined that the insulation layer of the metallic wire, the insulation layer on the test basin, the thermal contact resistance between the wire and insulation layer, and finite wire length all lead to inaccuracies in the hot wire method [5]. This is due to the fact that the mathematical model behind the transient hot wire method assumes that the device consists of an infinite wire located in an infinite domain with no need for insulation on either the wire or test basin. Because this ideal device cannot be designed, the corrections for each of these sources of inaccuracies have been researched significantly. The typical configuration for a hot wire cell is shown here in Figure 3.



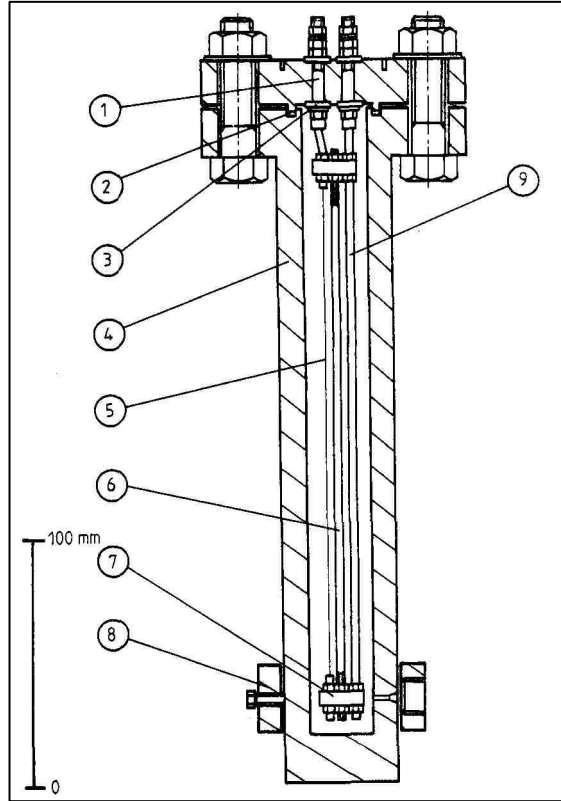


**Figure 3: Hot Wire Assembly, 1 – Terminal, 2 – Cu Packaging, 3 – Teflon Packing, 4 – Pressure Vessel, 5 – Insulated Pt Wire, 6 – Sus Rod, 7 – ABS Disk, 8 – Grand Retaining Ring, 9 – Insulated Cu Rod**

It is important to note the aspect ratio of the length of the wire compared to the diameter of the cell. If the aspect ratio is too low, then wall effects need to be considered when correcting the temperature data of the platinum wire. Therefore, in the design of these cells it is crucial that the cell diameter be large enough that wall effects are not a source of data inaccuracy.

In addition to the inaccuracies in the design of typical hot wire devices, the calibration used to calculate thermal conductivity is classically formulated using a one-term series solution to the infinite wire in an infinite medium problem. This problem is

well defined and the solution that is historically used is the one-term solution for large times. The problem with this calibration is that when the platinum wire is heated for large times ( $t > 1000$  s) the entire test medium temperature is affected, causing the test apparatus to heat. This evolving temperature field leads to convective heat transfer. Once natural convection begins, the calculation of an accurate thermal conductivity value is much more difficult. Therefore, the research herein demonstrates a method for measuring the thermal conductivity of liquids at high and low temperatures within a time period short enough that natural convection does not occur.

## Chapter 2: Measuring Thermal Conductivity

### 2.1 Definition of Thermal Conductivity

Thermal conductivity is a way to describe a material's ability to conduct heat. Fourier's law of heat conduction explains that the time rate of heat transfer through a material is proportional to the thermal conductivity, temperature gradient, and area of the material. Therefore, in order to successfully measure thermal conductivity, one must be able to measure the heat transfer and temperature gradient in the material being studied. Steady state and transient methods are primarily used to measure thermal conductivity.

### 2.2 Steady State Thermal Conductivity Measurement

Steady state thermal conductivity measurement techniques mainly apply to solids. The most popular steady state method of measuring thermal conductivity is the Divided Bar Method. This method has been used by geologists and material scientists to measure the thermal conductivity of solid materials using the principle of a constant temperature difference across the test material [9]. The temperature gradient across the test material is compared with that of a material with a known thermal conductivity. This comparison leads to the calculation of the thermal conductivity of the test material through the following formulation:

$$k_s = \frac{dk_g}{l\left(\frac{\Delta T_2}{\Delta T_1 + \Delta T_3}\right) - Rk_g} \quad (2.2.1)$$

Where  $k_s$  is the conductivity of the sample,  $k_g$  is the conductivity of the reference material,  $d$  is the thickness of the sample,  $l$  is the total thickness of the reference material, the three differential temperatures are the temperature differences across various parts of

the apparatus that are displayed in Figure 4, and  $R$  is the bar resistance which is determined by calibration.

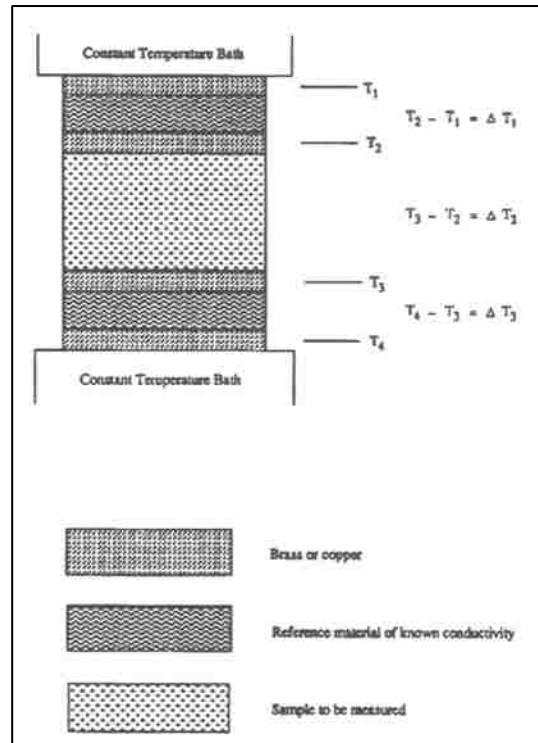


**Figure 4: Schematic of cross-section of divided-bar apparatus**

### 2.3 Transient Thermal Conductivity Measurement

Although steady state methods of measuring thermal conductivity are simple in theory, it is difficult to successfully engineer an apparatus that can apply truly steady state conditions. Therefore, although more difficult to model mathematically, transient methods of measuring thermal conductivity are chosen more frequently in order to successfully measure the thermal conductivity of solids and fluids. Three main methods of measuring thermal conductivity will be studied here.

First, the Transient Plane Source Method uses a flat sensor that typically utilizes nickel etched out of thin foil and clad between two layers of polyamide film Kapton. A current is passed through the nickel and creates a temperature rise in the test material. The sensor records the temperature vs. time response and the thermal properties of the material can then be derived from this data [10]. This method is easily applied to both solid and liquid samples and is typically used in the building industry to measure the thermal properties of building materials and other slurries.

The second method being studied is the Transient Line Source Method. This method is the most popular and frequently utilized method of measuring thermal conductivity. The ideal model of a transient line source device is an infinite line source with constant power per unit length that is applied to an infinite medium of test material. This ideal model can be used to solve for the temperature distribution in the material as a function of radial distance from the line source and time. The governing equation behind this model can be formulated as follows:

$$\rho c_p \frac{\partial T}{\partial t} = k \nabla^2 T + Q \quad (2.3.1)$$

Where  $\rho$  is density,  $c_p$  is specific heat capacity,  $T$  is temperature,  $t$  is time,  $k$  is thermal conductivity, and  $Q$  is heat generation. This equation has a solution in the following form for the transient line source method:

$$\Delta T(r_0, t) = \frac{q}{4\pi k} \left[ \ln \left( \frac{4at}{r_0^2 e^\gamma} \right) + \frac{r_0^2}{4at} - \frac{1}{4} \left( \frac{r_0^2}{4at} \right)^2 + \dots \right] \quad (2.3.2)$$

Where  $r_0$  is the wire radius,  $t$  is time,  $q$  is the heat flux per unit length of the wire,  $k$  is thermal conductivity,  $a$  is the test material thermal diffusivity, and  $\gamma$  is Euler's constant. The terms in the square brackets are the expansion of the exponential integral [11].

This solution for the temperature at the probe surface is typically used to calculate the temperature rise in the test material. Then, this temperature vs. time data is used to calculate the thermal conductivity of the test material according to the following derived relation:

$$k = \frac{q}{4\pi L} \frac{d \ln(t)}{dT} \quad (2.3.3)$$

Where  $q$  is the heat input into the wire of length  $l$ ,  $t$  is the time elapsed during testing, and  $T$  is the wire temperature.

The final, most recently employed method of transient thermal conductivity measurement is the laser flash method. This method measures the thermal diffusivity of a thin disc of the test material in the thickness direction. The laser creates a temperature rise produced by a short laser energy pulse. The temperature data is collected and the thermal conductivity can be calculated as follows:

$$k(T) = a(T)c_p(T)\rho(T) \quad (2.3.4)$$

Where  $k$  is the thermal conductivity of the test material,  $a$  is the thermal diffusivity of the test material,  $c_p$  is the specific heat capacity, and  $\rho$  is the density.

This method is applicable over a wide range of temperatures and for a wide range of materials. Therefore, it has been successfully applied to high temperature melts such as molten salts with mean deviations of about 3.8% [12]. The typical apparatus configuration for the laser flash method is shown below in Figure 5 [13].

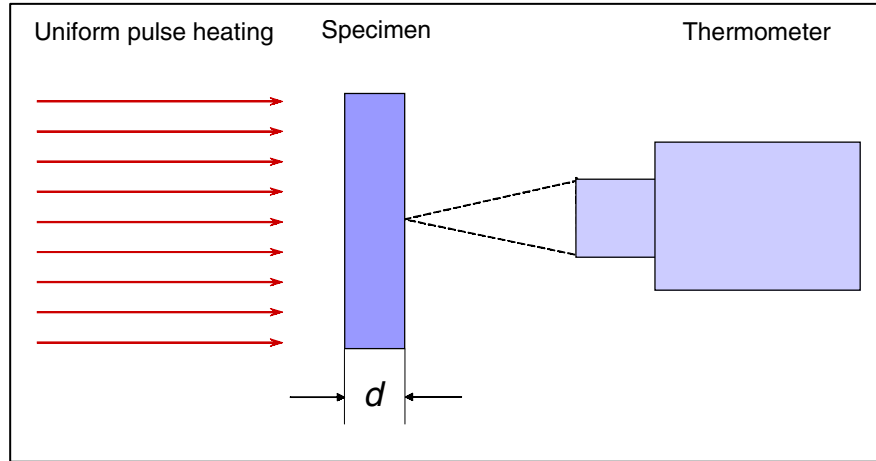


**Figure 5: Laser Flash Apparatus Design**

The current laser flash technology operates and collects accurate data under five important conditions. Firstly, the duration of the laser pulse must be negligibly short compared with the characteristic time of heat diffusion. Secondly, the laser pulse must uniformly heat the front face of the specimen. Thirdly, the specimen must be adiabatic during the measurement after the laser pulse is completed. Fourthly, the specimen must be geometrically uniform and homogeneous. Finally, the specimen must be opaque to the pulse of the laser and to thermal radiation. If these five conditions are met, then the analytic solution to the temperature in the specimen will be perfectly accurate. Due to the nature of conducting these experiments it is impossible to create an ideal environment where these five conditions are met. Therefore, there are inaccuracies in measuring the thermal conductivity of both solids and liquids with the laser flash technology.

#### **2.4 Choice of Measurement Technique for Current Research**

As described in the previous section, there are numerous ways to measure the thermal conductivity of both solids and liquids. Because the focus of the research

presented in this paper is the thermal conductivity of liquids, specifically molten salts, at elevated temperatures, a modified transient hot wire method is chosen. This choice is made for a few specific reasons. The transient hot wire device that is being used has been designed to operate at high temperatures. Also, because of the current inaccuracies in the laser flash method the transient hot wire method can be more easily calibrated for accurate results. A custom calibration is described in this paper because the current method of measuring temperature, as described in section 2.3, for most transient hot wire devices uses equation 2.3.2, but only with the choice of one term. Because a one-term solution is used, there are inaccuracies in the data analysis. The calibration described in this paper, coupled with the high accuracy of the Keithley source-meter and voltmeter being used, yields results in a shorter time period, with a higher order of accuracy than the current method of data acquisition and analysis.



## Chapter 3: Mathematical Model and Solutions

### 3.1 Theoretical Solution

In order to calculate the thermal conductivity of any medium with the transient hot wire device that is being used, a reliable and accurate calibration method needs to be determined. The device being used can be modeled as a platinum wire in an infinite cylindrical medium [14]. With the geometry shown below in Figure 6:

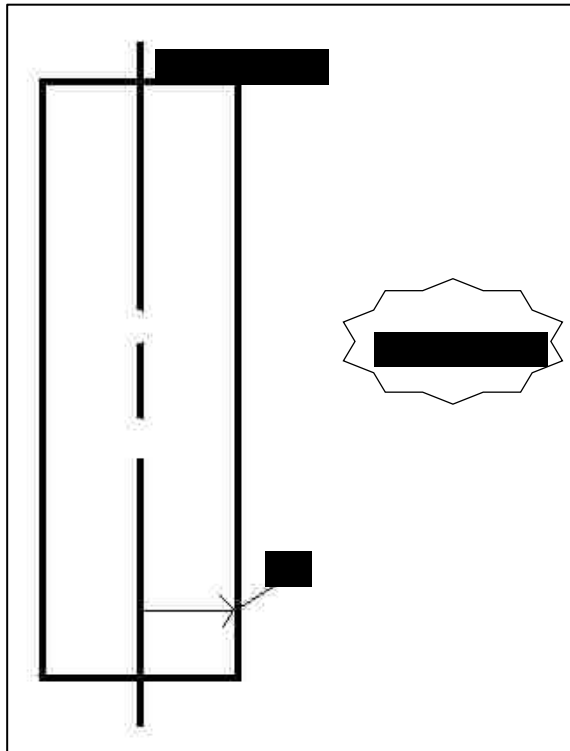


**Figure 6: Model Geometry**

A current will be passed through the wire, which will lead to a temperature increase in the wire. The measured resistance in the wire is converted to temperature and a temperature verses time plot is produced when performing the experiments. Therefore,

a way to calculate the thermal conductivity of the medium with this temperature versus time data needs to be established.

The device being used can be modeled using the one-dimensional, transient diffusion equation, in cylindrical coordinates. This equation is as follows:

$$\frac{\partial^2 T(r,t)}{\partial r^2} + \frac{1}{r} \frac{\partial T(r,t)}{\partial r} = \frac{1}{\alpha} \frac{\partial T(r,t)}{\partial t} \quad (3.1.1)$$

Where  $T(r,t)$  is the temperature of the platinum wire as a function of radius and time measured in degrees Kelvin,  $r$  is the radial distance from the center of the wire measured in meters,  $t$  is time measured in seconds, and  $\alpha$  is the thermal diffusivity of the medium measured in square meters per second.

This equation is subject to the following boundary conditions and initial condition:

$$1) r = r_0; -k \frac{\partial T}{\partial r} = Q \quad (3.1.2)$$

$$2) r \rightarrow \infty; T = 0 \quad (3.1.3)$$

$$3) t = 0; T = 0 \quad (3.1.4)$$

Boundary condition one states that at a radial value of  $r_0$  the derivative of temperature with respect to radius follows Fourier's law of conduction. Here  $r_0$  is the radius of the platinum wire measured in meters,  $k$  is the thermal conductivity of the medium measured in Watts per meter per degree Kelvin, and  $Q$  is the heat input into the platinum wire measured in Watts per square meter.

Boundary condition two states that as the radial distance from the center of the platinum wire approached infinity, the value of the temperature approaches zero or the initial temperature of the system.

The initial condition states that at the value of time equal to zero, the temperature is equal to zero or the initial temperature of the system.

In order to solve this equation for the temperature of the platinum wire interface with the medium, Laplace transforms will be utilized. First, proper scaling needs to be applied in order to manipulate the equation into a solvable form. The following non-dimensional variables are introduced in order to perform this manipulation:

$$R = \frac{r}{r_0}; \tau = \frac{\alpha}{r_0^2} t; \theta = \frac{k}{Qr_0} T \quad (3.1.5)$$

Where  $R$  is the non-dimensional length scale,  $\tau$  is the non-dimensional time scale, and  $\theta$  is the non-dimensional temperature scale. Applying these scaling variables, the governing equation becomes:

$$\frac{\partial^2 \theta(R, \tau)}{\partial R^2} + \frac{1}{R} \frac{\partial \theta(R, \tau)}{\partial R} = \frac{\partial \theta(R, \tau)}{\partial \tau} \quad (3.1.6)$$

This equation is subject to the following boundary conditions and initial condition:

$$1) R = 1; \frac{\partial \theta}{\partial R} = -1 \quad (3.1.7)$$

$$2) R \rightarrow \infty; \theta = 0 \quad (3.1.8)$$

$$3) \tau = 0; \theta = 0 \quad (3.1.9)$$

Now, Laplace transforms can be applied in order to solve the governing equation.

The Laplace transform of the temperature will be defined as:

$$\theta(R, s) = \int_0^{\infty} \theta(R, \tau) e^{-s\tau} d\tau \quad (3.1.10)$$

Therefore, the Laplace transform of the governing equation becomes:

$$\frac{\partial^2 \theta(R, s)}{\partial R^2} + \frac{1}{R} \frac{\partial \theta(R, s)}{\partial R} = s\theta \quad (3.1.11)$$

This equation has a solution in the form of:

$$\theta(R, s) = \theta_0(s) \frac{K_0(\sqrt{s}R)}{K_0(\sqrt{s})} \quad (3.1.12)$$

Where  $\theta_0(s)$  is the temperature at the interface of the wire and the medium as a function of time in the s-domain. This equation automatically satisfies the second boundary condition stated above, because the modified Bessel function,  $K_0$ , approaches zero as its argument approaches infinity. In order to apply the first stated boundary condition, the solution above needs to be differentiated with respect to  $R$ . Taking this derivative yields:

$$\frac{\partial \theta(R, s)}{\partial R} = \sqrt{s} \theta_0(s) \frac{K_1(\sqrt{s}R)}{K_0(\sqrt{s})} \quad (3.1.13)$$

Applying the boundary condition at the radial value of one yields:

$$-\frac{1}{s} = -\sqrt{s} \frac{K_1(\sqrt{s})}{K_0(\sqrt{s})} \theta_0(s) \quad (3.1.14)$$

Simplifying this equation and solving for the interface temperature gives the solution:

$$\theta_0(s) = \frac{1}{s^{3/2}} \frac{K_0(\sqrt{s})}{K_1(\sqrt{s})} \quad (3.1.15)$$

This equation is the well-documented equation for the temperature at the wire surface where constant heat flux per unit time per unit area is applied. This equation has

been transformed into the real time domain by Carslaw and Jaeger, and the integral form of the solution in the real time domain for large and small times is as follows [15]:

$$T = -\frac{2Q}{\pi k} \int_0^{\infty} (1 - e^{-\alpha u^2 t}) \frac{J_0(ur)Y_1(ur) - Y_0(ur)J_1(ur)}{u^2 [J_1^2(ur) + Y_1^2(ur)]} du \quad (3.1.16)$$

Where  $Q$  is the heat flux in the wire measured in Watts per meter,  $k$  is the thermal conductivity of the medium measured in Watts per meter per degree Kelvin,  $\alpha$  is the thermal diffusivity of the medium measured in square meters per second,  $t$  is time measured in seconds,  $r$  is the radius of the wire measured in meters, and  $u$  is the variable of integration.

This integral form of the temperature distribution at the wire interface as a function of time will yield accurate results, but cannot be used for curve fitting purposes when deriving thermal conductivity values from experimental data. Therefore, the solution in the s-domain is approximated by a polynomial series and then the inverse Laplace transform is taken in order to yield a usable solution.

In order for the inverse Laplace transform to be applied to this equation and then scale it back into the real time and temperature domains, it is approximated by a polynomial series. Maple is used to expand this function into a polynomial series. Below is the first four terms of the series in the s-domain:

$$\theta_0(s) = \left(\frac{1}{s}\right)^{3/2} - \frac{1}{2s^2} + \frac{3}{8}\left(\frac{1}{s}\right)^{5/2} - \frac{3}{8s^3} + \frac{63}{128}\left(\frac{1}{s}\right)^{7/2} + O\left(\frac{1}{s^4}\right) \quad (3.1.17)$$

The inverse Laplace transform of this series can now be easily applied, and yields the following series in the non-dimensional time domain:

$$\theta_0(\tau) = 2\sqrt{\frac{\tau}{\pi}} - \frac{1}{2}\tau + \frac{1}{2}\frac{\tau^{3/2}}{\sqrt{\pi}} - \frac{3}{16}\tau^2 + \frac{21}{80}\frac{\tau^{5/2}}{\sqrt{\pi}} \quad (3.1.18)$$

Finally, using the non-dimensional variables stated above, this equation is now transferred back into the real time and temperature domain. The final form of the solution to this problem is as follows:

$$T_0 = \frac{Qr_0}{k} \left[ 2\sqrt{\frac{\alpha t}{\pi r_0^2}} - \frac{1}{2}\frac{\alpha t}{r_0^2} + \frac{1}{2}\frac{\left(\frac{\alpha t}{r_0^2}\right)^{3/2}}{\sqrt{\pi}} - \frac{3}{16}\left(\frac{\alpha t}{r_0^2}\right)^2 + \frac{21}{80}\frac{\left(\frac{\alpha t}{r_0^2}\right)^{5/2}}{\sqrt{\pi}} + \dots \right] \quad (3.1.19)$$

This representation of the temperature at the wire-medium interface is used to calibrate the thermal conductivity-measuring device. Using this equation, the temperature versus time data taken from the device can be fit to a curve made with this equation, and then the thermal conductivity of the medium can be determined as it is the only unknown variable in the equation.

### 3.1.1 Theoretical Solution Sensitivity Analysis

The aforementioned final equation for the interface temperature as a function of time is represented by a series solution. Any number of terms can be taken in formulating this solution, but the correct number of terms needs to be used in order for the solution to be accurate for the correct period of time. The following analysis demonstrates the sensitivity of the series solution to the number of terms that are used.

In order to plot the series solution without the effect of the medium properties, the non-dimensional form of the solution is used for plotting in this section. The plot below details the behavior of the solution for three, seven, and fifteen terms.

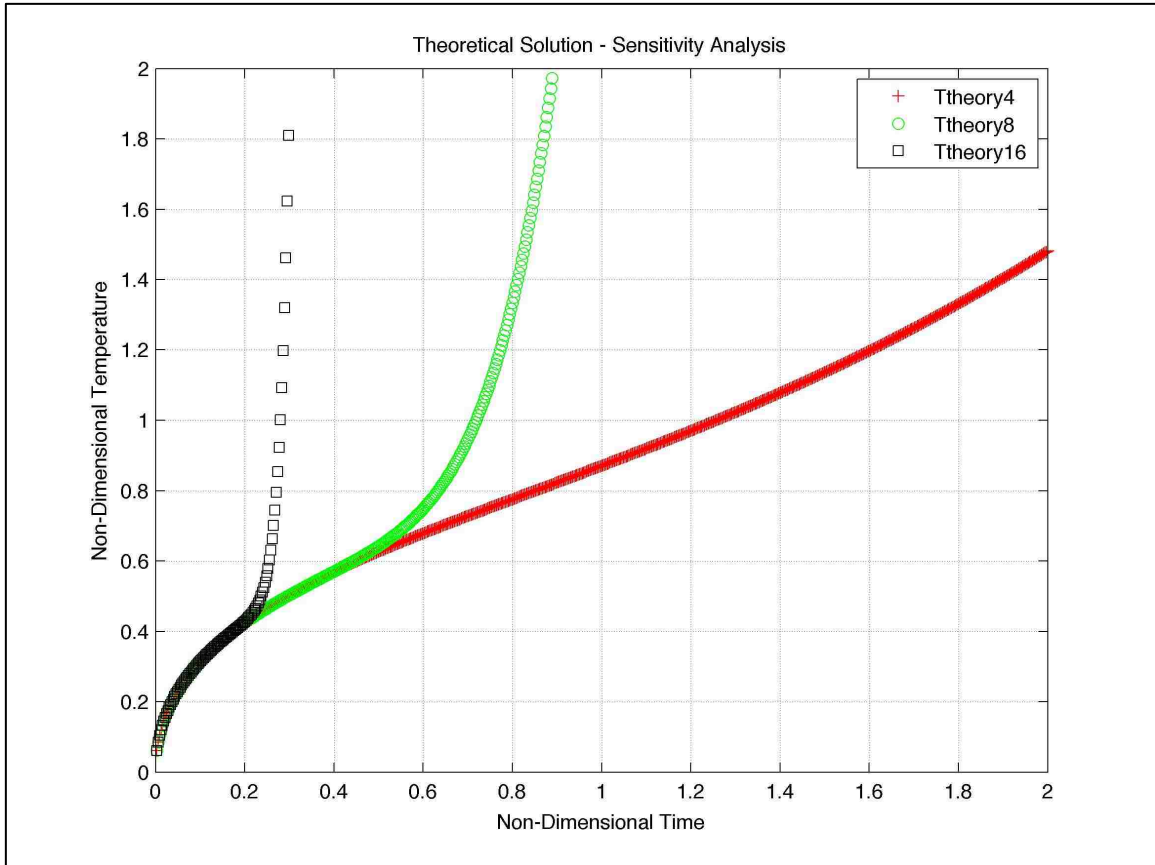


**Figure 7: Theoretical Sensitivity Analysis For "Long" Times**

In Figure 7 it is shown that from  $\tau$  from 0 to about 0.25 all three series solution yield identical results. At this point the series solution that utilizes fifteen terms begins to diverge from the solutions that utilize three and seven terms. Then at about 0.5 the solution with seven terms diverges in a similar fashion to that of the solution with fifteen terms. Then the three-term solution seems to continue on in a relatively linear fashion, but diverges from that path as well at larger times. Below, in Figure 8 is a closer look at the three different series.

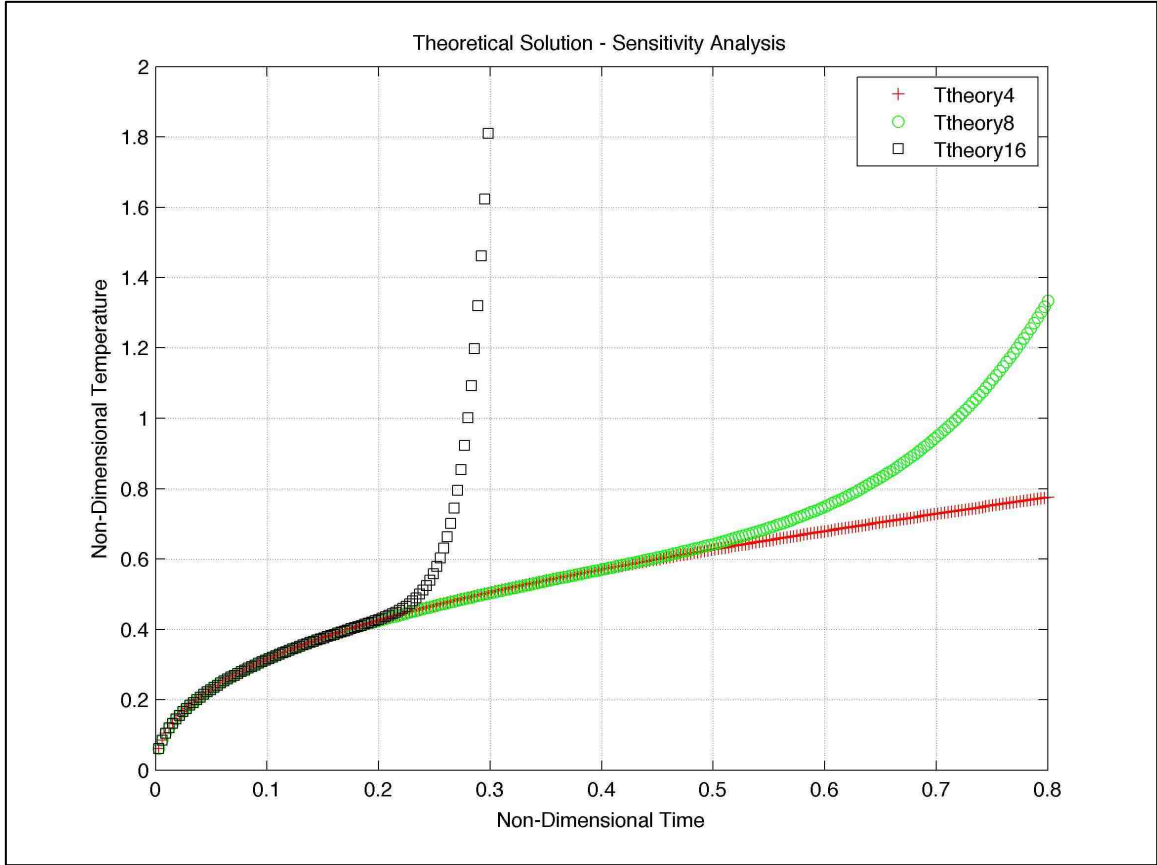


**Figure 8: Theoretical Sensitivity Analysis For "Short" Times**

Again, the divergence of the fifteen and seven term solutions from the three-term solution can be seen in Figure 8 with more detail. It is important to note that the three forms of the solution provide identical data up to about 0.2 on the  $\tau$ -axis.

In order to use the part of the solution that is accurate for the time of the experiment without diverging, the three-term series is chosen. A numerical solution to the same partial differential equation is demonstrated in the next section to prove the accuracy of the three-term series solution, but the following equation is the final form of the three-term solution to the partial differential equation above, when converted into the real time and real temperature domain:



$$T_0 = \frac{Qr_0}{k} \left[ 2 \sqrt{\frac{\alpha t}{\pi r_0^2}} - \frac{1}{2} \frac{\alpha t}{r_0^2} + \frac{1}{2} \frac{\left(\frac{\alpha t}{r_0^2}\right)^{3/2}}{\sqrt{\pi}} \right] \quad (3.1.20)$$

Where  $T$  is the temperature as a function of time at the wire/medium interface in degrees Celsius,  $Q$  is the heat input into the system in Watts per unit surface area (square meter) of wire,  $r_0$  is the wire radius in meters,  $k$  is the thermal conductivity of the medium in Watts per meter per degree Kelvin,  $\alpha$  is the thermal diffusivity of the medium in square meters per second, and  $t$  is time in seconds.

### 3.2 Numerical Simulation

In order to use the theoretical solution above, its accuracy must be proven. In order to do so, a numerical simulation is created to solve the same governing partial differential equation using the finite difference method. The governing equation is shown here:

$$\frac{\partial^2 \theta(R, \tau)}{\partial R^2} + \frac{1}{R} \frac{\partial \theta(R, \tau)}{\partial R} = \frac{\partial \theta(R, \tau)}{\partial \tau} \quad (3.2.1)$$

To solve this equation numerically, the method of finite differences is used to discretize this equation and its related boundary conditions. The discretization technique is shown here, as the governing equation becomes:

$$\frac{\theta_i^{n+1} - \theta_i^n}{\Delta \tau} = \frac{1}{R_i} \left[ \frac{\theta_{i+1}^n - \theta_{i-1}^n}{2\Delta R} \right] + \frac{\theta_{i+1}^n - 2\theta_i^n + \theta_{i-1}^n}{\Delta R^2} \quad (3.2.2)$$

This equation will define the temperature at each sequential time step for all interior nodes of the designed mesh. The boundary and initial conditions for this simulation are as follows:

$$1) \theta_i^1 = 0, \quad 2) \theta_i^n = 0, \quad 3) \frac{4\theta_2^n - \theta_3^n - 3\theta_1^n}{2\Delta R} = -1 \quad (3.2.3)$$

Where condition one is the initial condition stating that the temperature across the entire mesh at time is equal to zero is zero. The second condition states that the temperature at the radial value of infinity is equal to the initial temperature. Finally, the third condition is the discretized form of the conduction condition at the wire/medium interface in discretized for with second order error. The source code for this simulation is written in Maple and can be found in Appendix A.

### **3.3 Comparison of Numerical and Series Solutions**

Comparing the plots of the two solutions together compares the accuracy of the series solution demonstrated above to the numerical solution. The plot below displays the two solutions together in terms of non-dimensional variables, including the series solution with one, two, three, and seven terms to prove the most usable solution lies with the three-term solution.

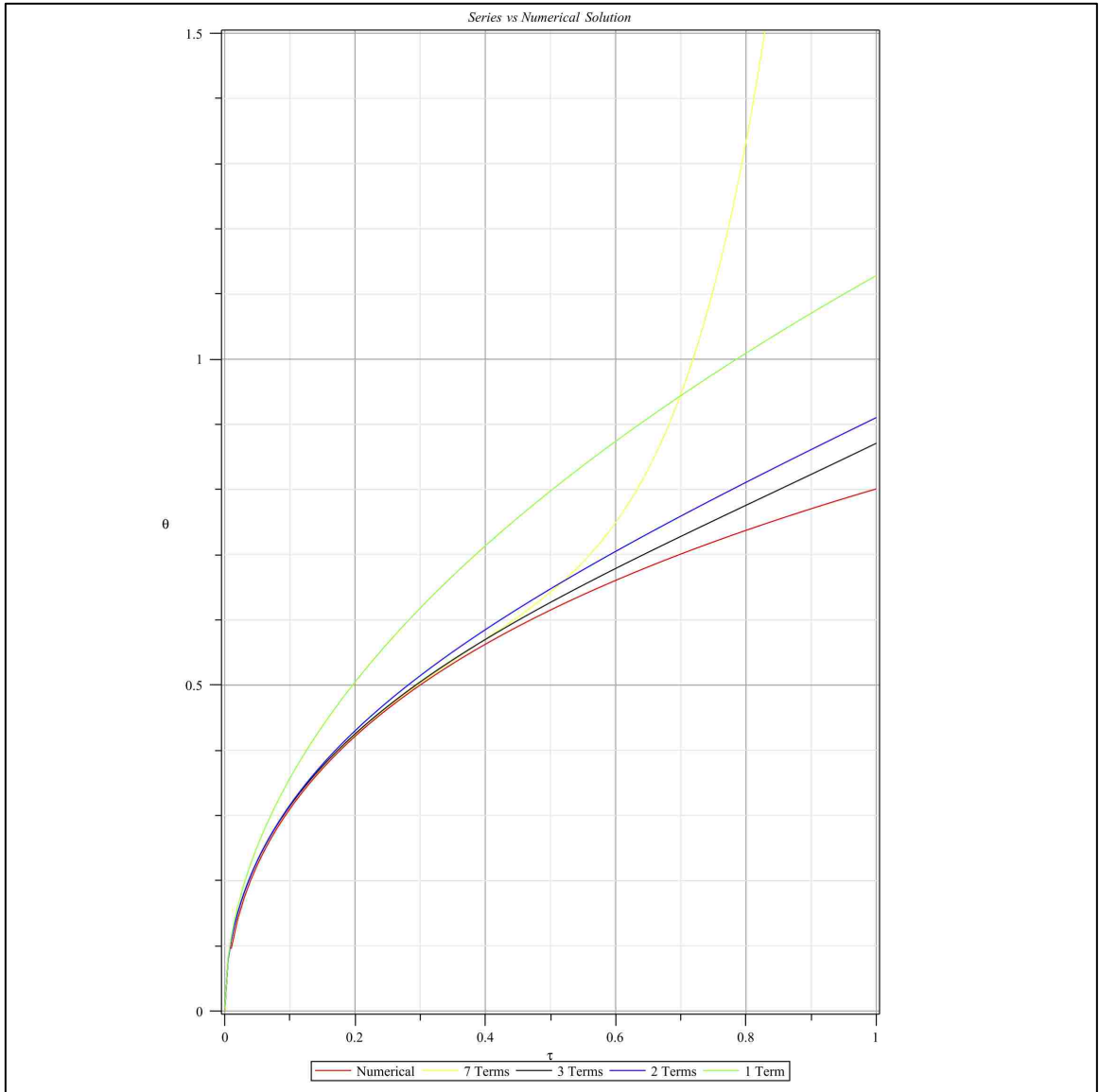


**Figure 9: Series Solution Plotted with Numerical Solution**

It is clearly demonstrated in Figure 9 that the three-term series solution and the numerical solution have the closest relation. This also demonstrates the validity of the series solution. Therefore, the three-term series solution can be used to calibrate the desired thermal conductivity-measuring device by curve fitting experimental data with the series solution.

## **Chapter 4: Experimental Analysis**

### **4.1 Calibration Experiment Procedure**

In order to determine the accuracy of the chosen thermal conductivity-measuring device, proper calibration experiments must be performed. Using liquids with well-documented properties will allow for this calibration and verification of results to be completed. It is proposed that verification experiments be performed on well-known liquids at varying temperatures to verify the devices response and results at both room temperature and elevated temperatures. This is because in order to measure the thermal conductivity of molten salts, the test temperatures can approach values above six hundred degrees Celsius.

The experimental procedure for testing the device will be as follows. First, the test liquid will be poured into the measuring device, which will then be placed in a temperature controlled environment at the desired initial testing temperature. Once the temperature probe in the test material shows that the entire system has reached equilibrium the test can begin. A current will be supplied to the circuitry, which will cause the platinum wire to heat. This will cause a temperature response in the test liquid. The platinum wire will also be used as a thermometer in order to measure the temperature at the wire/medium interface throughout the experiment. The temperature versus time data will be recorded in a LabVIEW program, which will then output a data file including the temperature verses time results. The slope of the results will then be curve fit to the slope of the three-term series solution described above. Using this equation, the thermal

conductivity of the test liquid can be determined, because it will be the only unknown variable in the formula. The slope, or derivative, of the series solution is as follows:

$$\frac{\partial T(t)}{\partial t} = \frac{Qr_0}{\sqrt{\rho c \pi r_0^2 k t}} - \frac{Q}{2\rho c r_0} + \frac{3Qk^{3/2}\sqrt{t}}{4\rho c r_0\sqrt{\pi}} \sqrt{\frac{1}{\rho c r_0^2}} \quad (4.1.1)$$

This procedure will be performed for water and propylene glycol at varying temperatures. These two liquids are chosen because their properties are well documented for a wide range of temperatures and can be used for calibration purposes.

## 4.2 Calibration Experiments

### 4.2.1 Water at 23 Degrees Celsius

This experiment is performed on water at 23 degrees Celsius. The parameters and properties of the experiment are as follows:

Property	Value
Thermal Conductivity, $k$ [W/m-K]	0.604 [16]
Specific Heat, $c$ [J/kg-K]	4.145 [16]
Density, $\rho$ [kg/m <sup>3</sup> ]	997.5 [16]
System Power, $P$ [W]	0.0270

**Table 1: Property Table for Water at 23 C**

Using the properties listed in Table 1, the following temperature response plot was created using the series solution and experimental data:

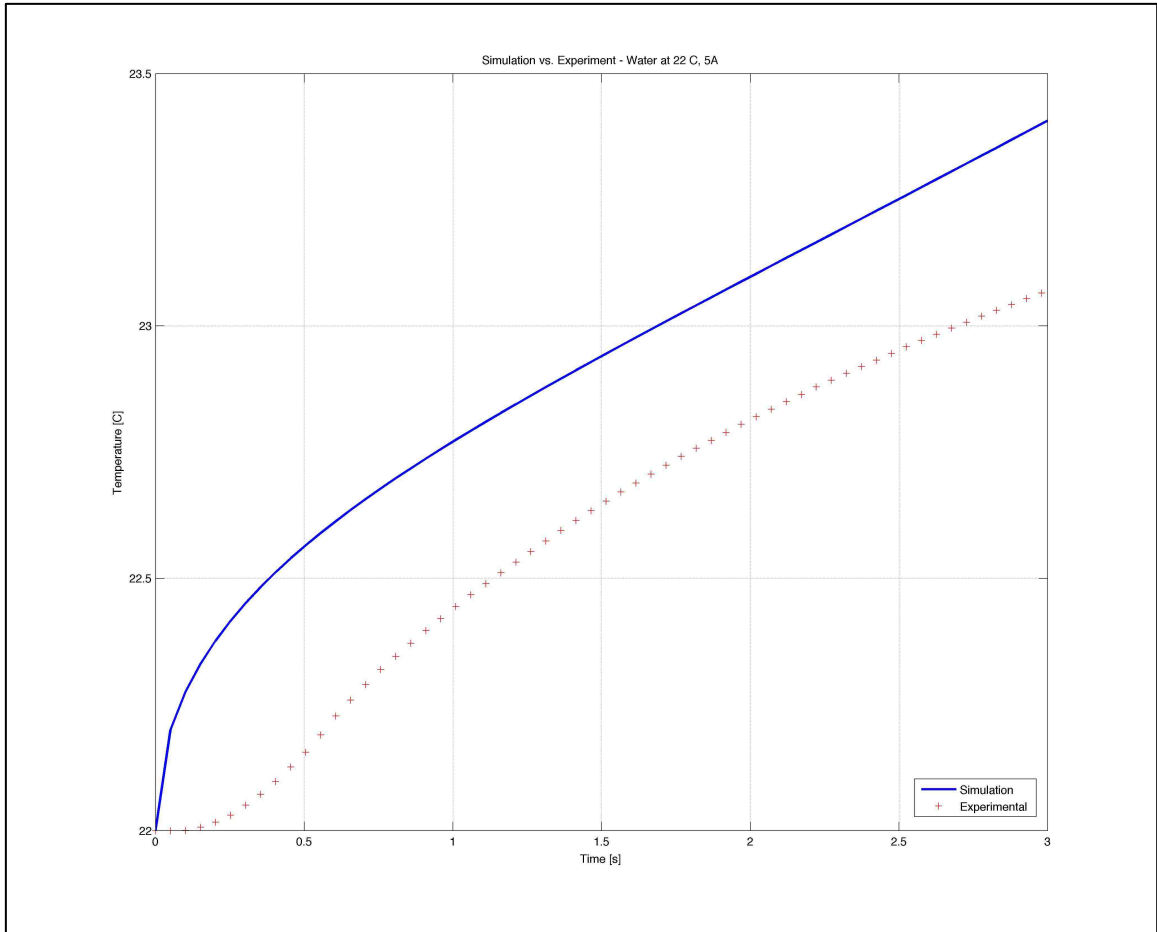


**Figure 10: Temperature Response of Water at 23 C**

As demonstrated in Figure 10, it is shown that the temperature response of the fluid in the experiment has a lag compared to the series solution. Although this is the case, the slope of the two curves can be compared to calculate the thermal conductivity of the test liquid using the experimental results. Below, the slope of the two curves are compared:

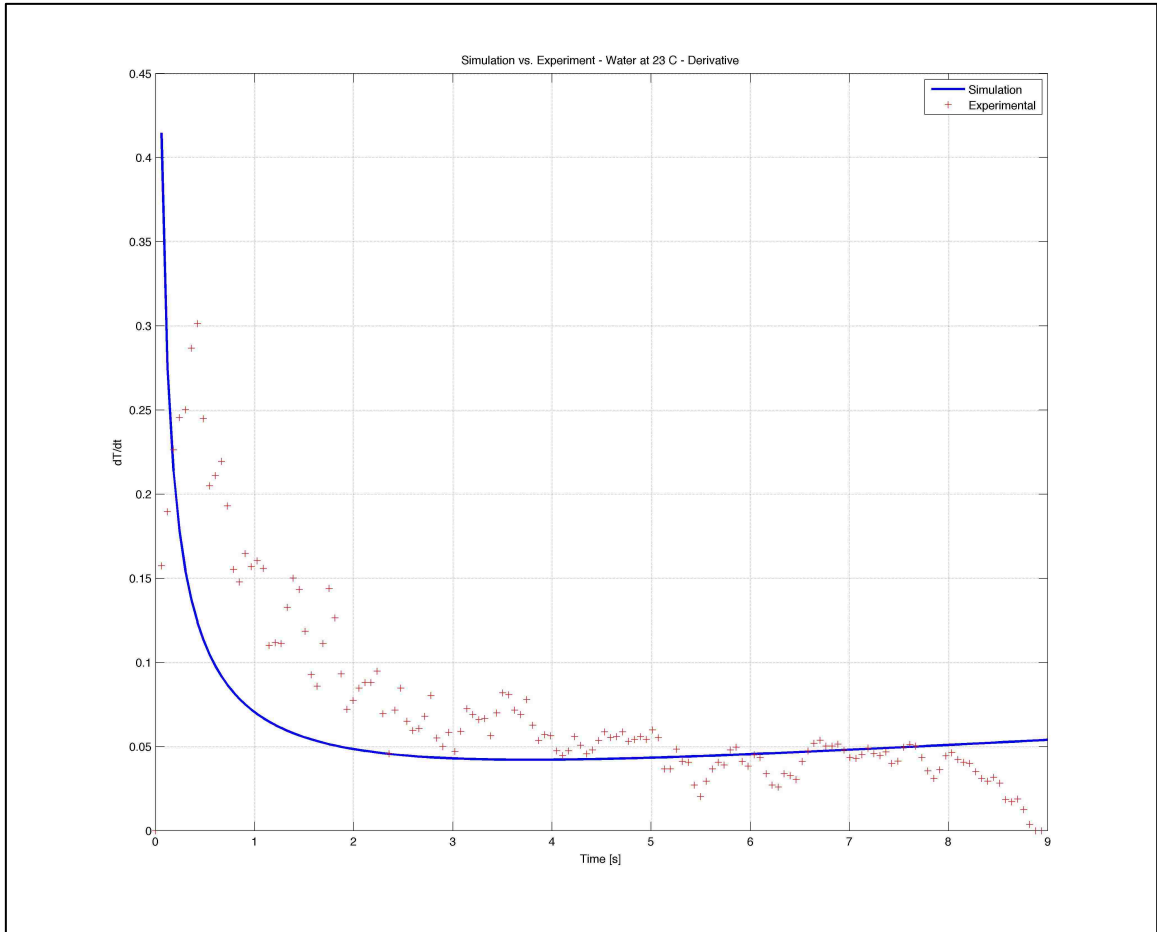


**Figure 11: Slope Comparison of Experimental Data to Series Solution for Water at 23 C**

In Figure 11 it is shown that the slope of the two curves, after the initial lag, is comparable. Because this is part of the device calibration, the portion of the data that matches most closely to the series solution will be used to calculate the thermal conductivity of the liquid. Therefore, between 6.5 and 7.5 seconds will be considered in the thermal conductivity calculation.

Using a non-linear least squares fit custom curve-fitting program written in MATLAB, which can be found in Appendix B, the thermal conductivity of the test liquid is calculated.

The summary of results from the three trials at this temperature is as follows:

<b>Trial</b>	<b>Calculated Thermal Conductivity, <math>k</math> [W/m-K]</b>	<b>% Error</b>
1	0.617	2.1
2	0.617	2.1
3	0.586	3.1
4	0.597	1.1

**Table 2: Summary of Results for Water at 23 C**

#### 4.2.2 Propylene Glycol at 24 Degrees Celsius

This experiment is performed on propylene glycol at 24 degrees Celsius. Three trials are performed at this temperature in order to determine the repeatability of the results. The parameters and properties of the experiment are as follows, and the analysis for one trial is explained below.

<b>Property</b>	<b>Value</b>
Thermal Conductivity, $k$ [W/m-K]	0.200 [17]
Specific Heat, $c$ [J/kg-K]	2.51 [17]
Density, $\rho$ [kg/m <sup>3</sup> ]	1,032 [17]
System Power, $P$ [W]	0.249

**Table 3: Property Table for Propylene Glycol at 24 C**

Using the properties listed in Table 3, the following temperature response slope plot was created using the series solution and experimental data:



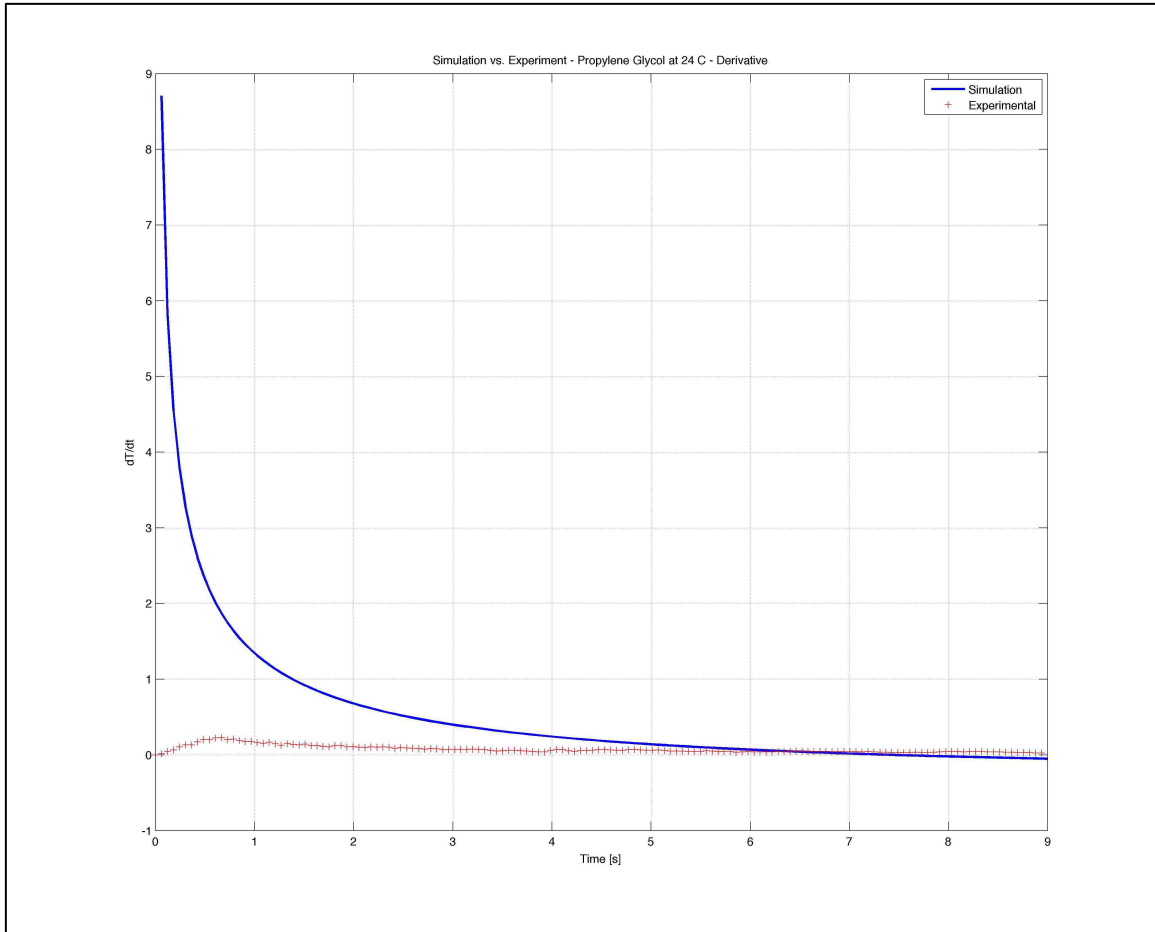


**Figure 12: Temperature Response Slope of Propylene Glycol at 24 C**

As demonstrated in Figure 12, it is shown that the temperature response slope of the fluid in the experiment and the slope of the series solution converge to a similar value 5.5 and 7 seconds of heating. Therefore, the data between 5.5 and 7 seconds is used in calculating the thermal conductivity of the propylene glycol.

Using the non-linear least squares fit custom curve-fitting program written in MATLAB, which can be found in Appendix B, the thermal conductivity of the test liquid is calculated.

The summary of results from the three trials at this temperature is as follows:

<b>Trial</b>	<b>Calculated Thermal Conductivity, <math>k</math> [W/m-K]</b>	<b>% Error</b>
1	0.220	10.1
2	0.210	5.0
3	0.213	6.7

**Table 4: Summary of Results for Propylene Glycol at 100 C**

Here it is shown that the percent error for each trial is between five and ten percent when compared to the documented literature value.

#### **4.2.3 Propylene Glycol at 60 Degrees Celsius**

This experiment is performed on propylene glycol at 60 degrees Celsius. Three trials are performed at this temperature in order to determine the repeatability of the results. The parameters and properties of the experiment are as follows, and the analysis for one trial is explained below.

<b>Property</b>	<b>Value</b>
Thermal Conductivity, $k$ [W/m-K]	0.1996 [17]
Specific Heat, $c$ [J/kg-K]	2.51 [17]
Density, $\rho$ [kg/m <sup>3</sup> ]	928.2 [17]
System Power, $P$ [W]	0.256

**Table 5: Property Table for Propylene Glycol at 60 C**

Using the properties listed in Table 5, the following temperature response slope plot was created using the series solution and experimental data:

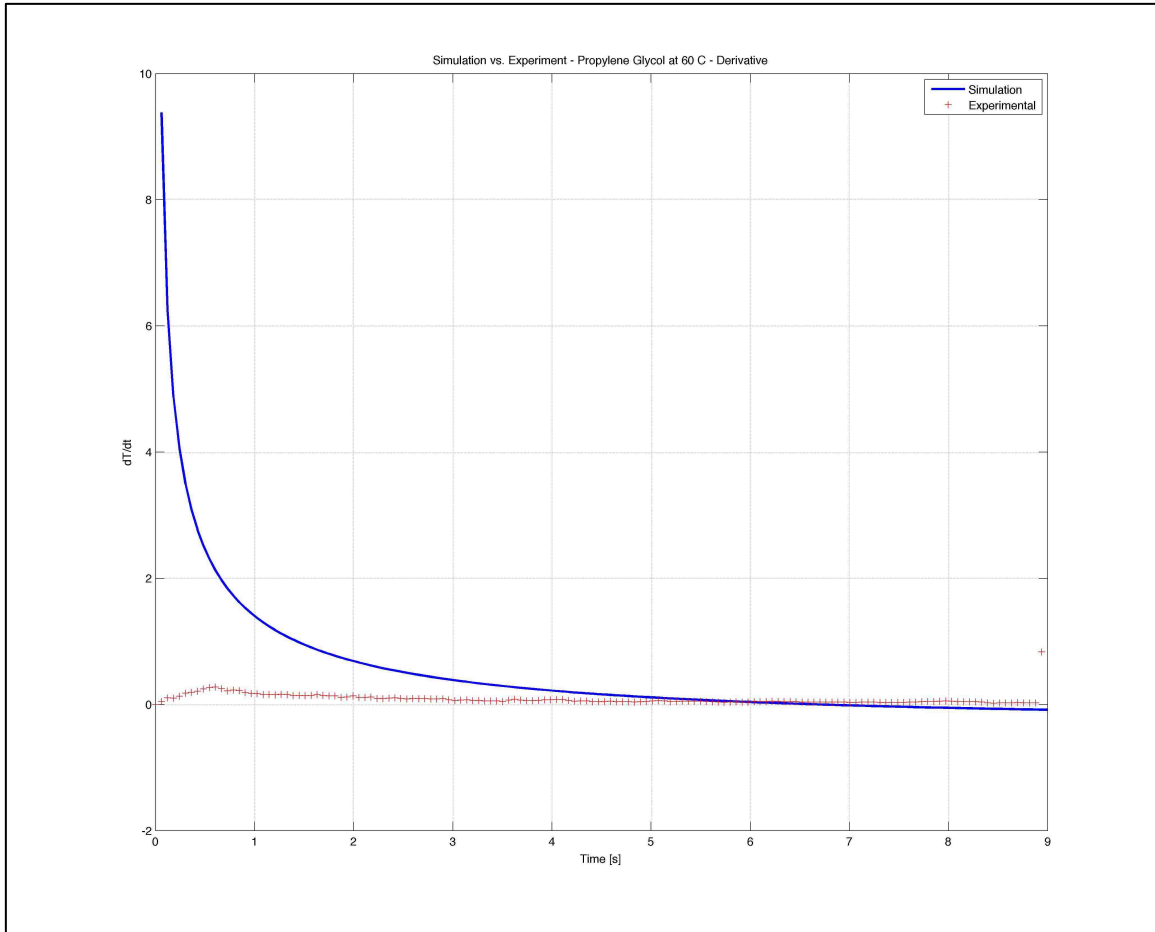


**Figure 13: Temperature Response Slope of Propylene Glycol at 60 C**

As demonstrated in Figure 13, it is shown that the temperature response slope of the fluid in the experiment and the slope of the series solution converge to a similar value between 5.5 and 7 seconds of heating. Therefore, the data between 5.5 and 7 seconds is used in calculating the thermal conductivity of the propylene glycol.

Using the non-linear least squares fit custom curve-fitting program written in MATLAB, which can be found in Appendix B, the thermal conductivity of the test liquid is calculated.

The summary of results from the three trials at this temperature is as follows:

<b>Trial</b>	<b>Calculated Thermal Conductivity, <math>k</math> [W/m-K]</b>	<b>% Error</b>
1	0.227	13.8
2	0.211	5.9
3	0.221	10.9

**Table 6: Summary of Results for Propylene Glycol at 60 C**

Here it is shown that the percent error for each trial is between five and fourteen percent when compared to the documented literature value.

#### **4.2.4 Propylene Glycol at 80 Degrees Celsius**

This experiment is performed on propylene glycol at 80 degrees Celsius. Three trials are performed at this temperature in order to determine the repeatability of the results. The parameters and properties of the experiment are as follows, and the analysis for one trial is explained below.

<b>Property</b>	<b>Value</b>
Thermal Conductivity, $k$ [W/m-K]	0.1986 [17]
Specific Heat, $c$ [J/kg-K]	2.51 [17]
Density, $\rho$ [kg/m <sup>3</sup> ]	901.8 [17]
System Power, $P$ [W]	0.262

**Table 7: Property Table for Propylene Glycol at 80 C**

Using the properties listed in Table 7, the following temperature response slope plot was created using the series solution and experimental data:

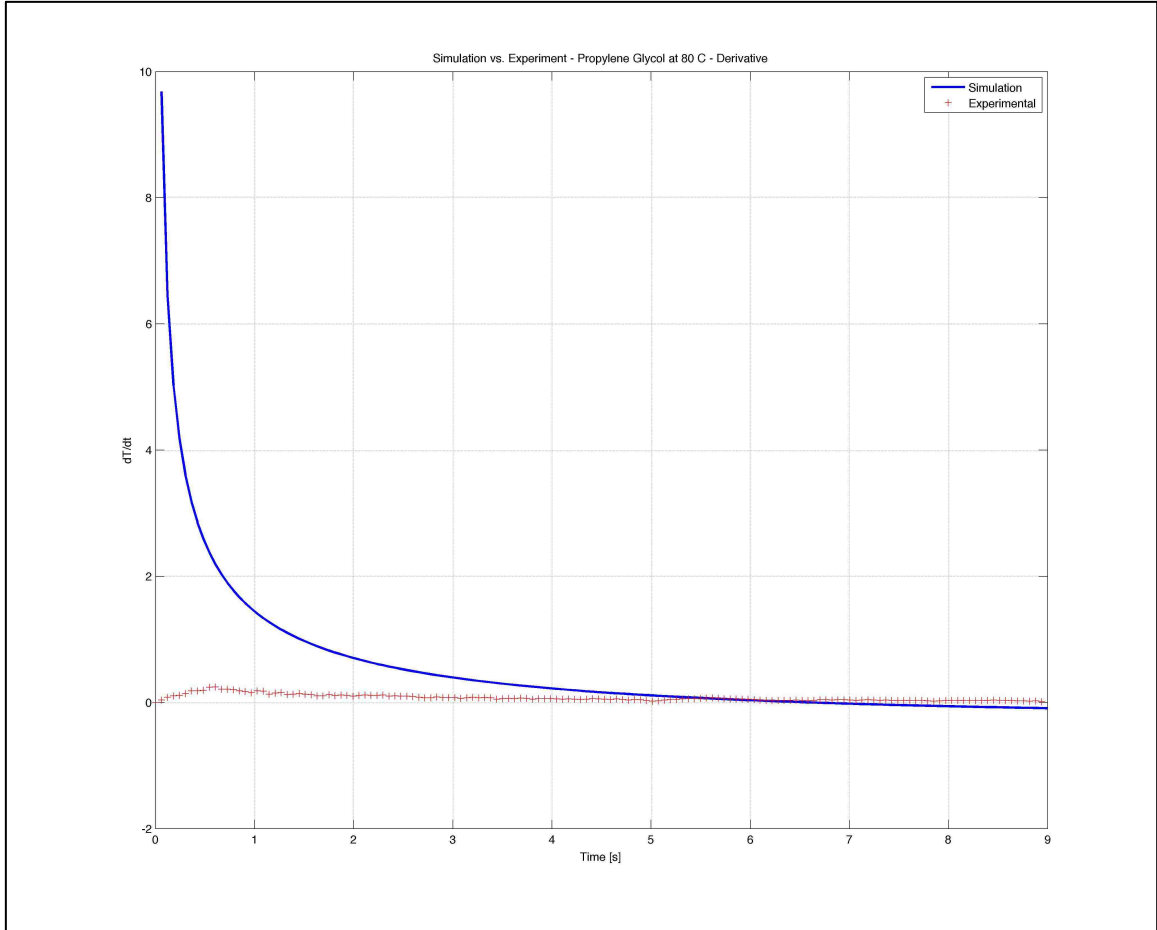


**Figure 14: Temperature Response Slope of Propylene Glycol at 80 C**

As demonstrated in Figure 14, it is shown that the temperature response slope of the fluid in the experiment and the slope of the series solution converge to a similar value between 5.5 and 6.75 seconds of heating. Therefore, the data between 5.5 and 6.75 seconds is used in calculating the thermal conductivity of the propylene glycol.

Using the non-linear least squares fit custom curve-fitting program written in MATLAB, which can be found in Appendix B, the thermal conductivity of the test liquid is calculated.

The summary of results from the three trials at this temperature is as follows:

<b>Trial</b>	<b>Calculated Thermal Conductivity, <math>k</math> [W/m-K]</b>	<b>% Error</b>
1	0.236	18.9
2	0.215	8.3
3	0.214	8.1

**Table 8: Summary of Results for Propylene Glycol at 100 C**

Here it is shown that the percent error for each trial is between eight and twenty percent when compared to the documented literature value.

#### **4.2.5 Propylene Glycol at 100 Degrees Celsius**

This experiment is performed on propylene glycol at 100 degrees Celsius. Three trials are performed at this temperature in order to determine the repeatability of the results. The parameters and properties of the experiment are as follows, and the analysis for one trial is explained below.

<b>Property</b>	<b>Value</b>
Thermal Conductivity, $k$ [W/m-K]	0.1968 [17]
Specific Heat, $c$ [J/kg-K]	2.51 [17]
Density, $\rho$ [kg/m <sup>3</sup> ]	901.8 [17]
System Power, $P$ [W]	0.268

**Table 9: Property Table for Propylene Glycol at 100 C**

Using the properties listed in Table 9, the following temperature response slope plot was created using the series solution and experimental data:

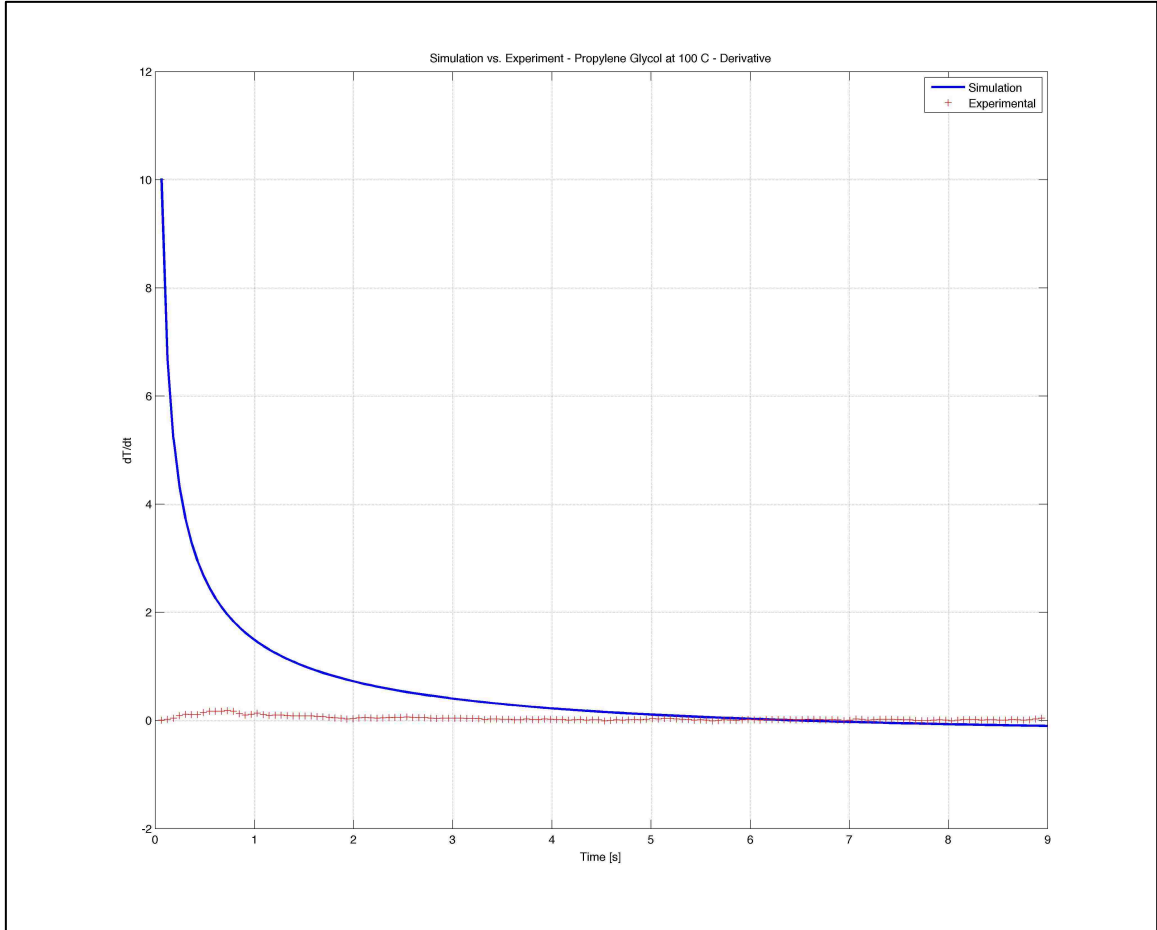


**Figure 15: Temperature Response Slope of Propylene Glycol at 100 C**

As demonstrated in Figure 15, it is shown that the temperature response slope of the fluid in the experiment and the slope of the series solution converge to a similar value 5.75 and 7 seconds of heating. Therefore, the data between 5.75 and 7 seconds is used in calculating the thermal conductivity of the propylene glycol.

Using the non-linear least squares fit custom curve-fitting program written in MATLAB, which can be found in Appendix B, the thermal conductivity of the test liquid is calculated.

The summary of results from the three trials at this temperature is as follows:

<b>Trial</b>	<b>Calculated Thermal Conductivity, <math>k</math> [W/m-K]</b>	<b>% Error</b>
1	0.207	5.4
2	0.222	12.8
3	0.205	4.2

**Table 10: Summary of Results for Propylene Glycol at 100 C**

Here it is shown that the percent error for each trial is between five and thirteen percent when compared to the documented literature value.

#### **4.4 Summary of Calibration Experiments**

As described in the calibration experiments for both water and propylene glycol, it is shown that the thermal conductivity of the test medium can be calculated using the slope of the experimental temperature data. It is found that the properties of the test material are closely related to the portion of heating time that should be used for the thermal conductivity calculation. With water, as shown above, between 5 and 7 seconds is used, and a percent error of less than 3% is found for all trials. With the propylene glycol the liquid needs to be heated for 9 seconds in order for the experimental and theoretical data to converge to a similar value. Even with 9 seconds of heating the percent error in all propylene glycol cases can be as high as 18.9 % and as low as 4.2 %.

The main source of error in these results is the temperature control of the test environment. The furnace being used cannot control the ambient temperature accurately enough to get the proper data necessary. The reason the temperature control is determined to be the main source of error is because the room temperature results are most accurate. For water, at room temperature the percentages of error are less than 3% but as high as 19% for the propylene glycol at an elevated controlled temperature.



Therefore, it is suggested that a more accurately controlled furnace be obtained to perform these experiments. Also, a multitude of calibration liquids, with well-known properties should be tested in order to determine the range of time in which the test data should be analyzed. The factors that should be considered in this analysis are the specific heat and density of the liquid, as these two properties must be known for the thermal conductivity of any liquid to be measured with this device.

## Chapter 5: Summary and Conclusions

After analyzing the mathematical model of the infinite wire in the test liquid medium, an accurate analytic solution has been found to model the temperature profile at the platinum wire interface. This formulation can now be used to calibrate the thermal conductivity-measuring device and then measure the thermal conductivity of any test liquid over a wide range of temperatures. The solution that has been found is in the following form:

$$T_0 = \frac{Qr_0}{k} \left[ 2 \sqrt{\frac{\alpha t}{\pi r_0^2}} - \frac{1}{2} \frac{\alpha t}{r_0^2} + \frac{1}{2} \frac{\left(\frac{\alpha t}{r_0^2}\right)^{3/2}}{\sqrt{\pi}} \right]$$

Where  $T$  is the temperature as a function of time at the wire/medium interface in degrees Celsius,  $Q$  is the heat input into the system in Watts per cubic meter of wire,  $r_0$  is the wire radius in meters,  $k$  is the thermal conductivity of the medium in Watts per meter per degree Kelvin,  $\alpha$  is the thermal diffusivity of the medium in square meters per second, and  $t$  is time in seconds.

This solution has been verified with a numerical simulation, which is described in section 2.3. In section 2.3 it is demonstrated that the numerical solution matches the analytic solution sufficiently. Because this solution is verified, it is then used to curve fit the experimental data of the calibration experiments explained above.

It was found that the properties of the test material are closely related to the portion of heating time that should be used for the thermal conductivity calculation. With water, as shown above, between 5 and 7 seconds of heating time is used, and a percent

error of less than 3% is found for all trials. With the propylene glycol the liquid needs to be heated for 9 seconds in order for the experimental and theoretical data to converge to a similar value. Even with 9 seconds of heating the percent error in all propylene glycol cases can be as high as 18.9 % and as low as 4.2 %.

The main source of error in these results is the temperature control of the test environment. The furnace being used cannot control the ambient temperature accurately enough to get the proper data necessary. The reason the temperature control is determined to be the main source of error is because the room temperature results are most accurate. For water, at room temperature the percentages of error are less than 3% but as high as 19% for the propylene glycol at an elevated controlled temperature.

Therefore, it is suggested that a more accurately controlled furnace be obtained to perform these experiments. Also, a multitude of calibration liquids, with well-known properties should be tested in order to determine the range of time in which the test data should be analyzed. The factors that should be considered in this analysis are the specific heat and density of the liquid, as these two properties must be known for the thermal conductivity of any liquid to be measured with this device.

## References

- [1] H. Bloom, A. Doroszkowski, S.B. Tricklebank. *Aust. J. Chem.*, Vol. 18, pp. 1171 (1965)
- [2] L.R. White. Doctoral Dissertation, University of Minnesota (1967)
- [3] A.G. Turnbull. *Aust. J. Appl. Sci.*, Vol. 12, pp. 324 (1961)
- [4] J. McDonald, H.T. Davis. *Thermal Conductivity of Binary Mixtures of Alkali Nitrates*. Dept. of Chemical Engineering, University of Minnesota, Minneapolis, Minnesota (1969)
- [5] Y. Nagasaka, A. Nagashima. *Absolute Measurement of the Thermal Conductivity of Electrically Conducting Liquids by the Transient Hot-Wire Method*. *J. Phys. E: Sci. Instrum.*, Vol. 14, pp. 1435-1440 (1981)
- [6] J.F. Pittman. *Fluid Thermal Conductivity Determination by the Transient Line Source Method*. PhD Thesis. University of London (1968)
- [7] J.W. Haarman. *An Accurate Method for the Determination of the Thermal Conductivity of Gases*. PhD Thesis. Technische Hogeschool, Delft (1969)
- [8] N. Mani. *Precise Determination of the Thermal Conductivity of Fluids Using Absolute Transient Hot-Wire Technique*. PhD Thesis. University of Calgary, Canada (1971)
- [9] F.W. Jones, F. Pascal. *Numerical Simulation of Divided-Bar Thermal Conductivity Measurements* (1991)

- [10] D. Bentz, Transient Plane Source Measurements of Thermal Properties of Hydrating Cement Pastes. *Materials and Structures Journal*, Vol. 40, No. 10, pp. 1073-1080 (2007)
- [11] J. Bilek, J.K. Atkinson, W.A. Wakeham. Repeatability and Refinement of a Transient Hot Wire Instrument for Measuring the Thermal Conductivity of High Temperature Melts. *International Journal of Thermophysics*, Vol. 27, No. 6, pp. 1626-1637 (2006)
- [12] Y. Tada, M. Harada, M. Tanigaki, W. Eguchi. Flash Method for Measuring Thermal Conductivity of Liquids. *Ind. Eng. Chem. Fundamentals*, Vol. 20, pp. 333-336 (1981)
- [13] T. Baba, A. Ono. Improvement of the Laser Flash Method to Reduce Uncertainty in Thermal Diffusivity Measurements. *Meas. Sci. Technol.*, Vol. 12, pp. 2046-2057 (2001)
- [14] S. Nelle. A Device for Measuring Thermal Conductivity of Molten Salt Nitrates at Elevated Temperatures for Use in Solar Thermal Power Applications. Lehigh University (2012)
- [15] H. S. Carslaw, J. C. Jaeger. *Conduction of Heat in Solids*. Second Edition, pp. 338 (1959)
- [16] Lide, D. R. (Ed.). *CRC Handbook of Chemistry and Physics*. (87th ed.) CRC Press (2006)
- [17] James, A. M. and M. P. Lord. *Macmillan's Chemical and Physical Data*. Macmillan (1992)

## Appendix A – Numerical Solution of Governing PDE

Numerical solution to partial differential equation governing the heat transfer in the thermal conductivity measuring device wire, written in Maple 14:

```
> restart; with(plots);

> dt := 0.1e-1; f0 := proc (r) options operator, arrow; 0*r end proc;

> for i to 100 do sln := dsolve({diff(f(r), r, r)+(diff(f(r), r))/r = (f(r)-f0(r))/dt, f(10) = 0,
(D(f))(1) = -1}, {f(r)}, numeric, output = listprocedure); f0 := subs(sln, f(r)); f1[i] := f0(1)
end do;

> plot([seq([i*dt, f1[i]], i = 1 .. 100)]);

> `&theta;series2` := 1.128379167*sqrt(tau)-.5000000000*tau+.2820947918*tau^(3/2);

> plot(`&theta;series2`, tau = 0 .. 1);

> p1 := plot([seq([i*dt, f1[i]], i = 1 .. 100)], color = "red");

> p2 := plot(`&theta;series2`, tau = 0 .. 1, color = "blue");

> `&theta;series3` := 1.128379167*sqrt(tau)-.5000000000*tau+.2820947918*tau^(3/2)-
.1875000000*tau^2+.1480997657*tau^(5/2);

> p3 := plot(`&theta;series3`, tau = 0 .. 1, color = "black");

> `&theta;series1` := 1.128379167*sqrt(tau);

> p4 := plot(`&theta;series1`, tau = 0 .. 1, color = "green");

> `&theta;series7` := 1.128379167*sqrt(tau)-.5000000000*tau+.2820947918*tau^(3/2)-
.1875000000*tau^2+.1480997657*tau^(5/2)-
.1406250000*tau^3+.1594339314*tau^(7/2)-
.2109375000*tau^4+.3168686419*tau^(9/2)-
.5277832031*tau^5+.9573817389*tau^(11/2)-
1.866741943*tau^6+3.874960991*tau^(13/2);

> p5 := plot(`&theta;series7`, tau = 0 .. 1, color = "yellow");

> display({p1, p2, p3, p4, p5}, axes = boxed, scaling = constrained, title =
'Series*vs*Numerical*Solution');
```

## Appendix B – Curve Fitting and Data Analysis

MATLAB code written to curve fit experimental data to series solution and calculate the thermal conductivity of the test liquids

```
clear all
clc

N=100;
Ttheory2=zeros(N,1);
Texp=zeros(N,1);
Ttp=zeros(N,1);
Tep=zeros(N-2,1);
t=zeros(N,1);
tep=zeros(N-2,1);

%%%%%%%%%%%%%% Parameter Input %%%%%%%%%%%%%%%

k=0.602;
rho=997.8;
c=4149;
alpha=k/(rho*c);
r=0.5*10^-3;
L=25.6*10^-3;
V=pi*L*r^2;
q=5.342*10^6;
P=q*V;
Q=P/(2*pi*r*L);
Ti=22;

%%%%%%%%%%%%%% Experimental Data %%%%%%%%%%%%%%%

load data.txt;

for i=1:1:N
    t(i,1)=data(i,1);
    Texp(i,1)=data(i,2);
end

dt=t(2)-t(1);

%%%%%%%%%%%%%% Series Solution %%%%%%%%%%%%%%%

for i=1:1:N
```

```

Ttheory2(i,1)=(2*sqrt(alpha*t(i)/(pi*r^2))-(1/2)*alpha*t(i)/r^2+...
(1/(2*sqrt(pi)))*(alpha*t(i)/r^2)^(3/2))*Q*r/k+Ti;
Ttp(i,1)=Q*r/sqrt(rho*c*pi*r^2)*1/sqrt(k)*1/sqrt(t(i))-...
Q/(2*rho*c*r)+3*Q/(4*sqrt(pi)*rho*c*r)*sqrt(1/(rho*c*r^2))*...
k^(3/2)*sqrt(t(i));
end

figure(1)
plot(t,Ttheory2,'LineWidth',2);
hold on
plot(t,Texp,'r+');
axis([0 3 22 23.5]);
title('Simulation vs. Experiment - Water at 22 C, 5A');
xlabel('Time [s]');
ylabel('Temperature [C]');
legend('Simulation', 'Experimental');
grid on;

%%%%%%%%%%%%%%%%%%%%%%%%%%%%%%%%%%%%%%%%%%%%%%%%%%%%%%%%%%%%%%%%%%%%%%%% Numerical Derivative of Experimental Data %%%%%%%%%

for i=2:1:N-1
    Tep(i,1)=(Texp(i+1)-Texp(i-1))/(2*dt);
end

for i=2:1:N-1
    tep(i,1)=t(i);
end

[C,I]=max(Tep);

figure(2)
plot(t,Ttp,'LineWidth',2);
hold on
plot(tep,Tep,'r+');
title('Simulation vs. Experiment - Water at 22 C, 5A - Derivative');
xlabel('Time [s]');
ylabel('dT/dt');
legend('Simulation', 'Experimental');
grid on;

%%%%%%%%%%%%%%%%%%%%%%%%%%%%%%%%%%%%%%%%%%%%%%%%%%%%%%%%%%%%%%%%%%%%%%%% Curve Fitting %%%%%%%%%

start=round(3.75*N/5);

```



```

a1=Q*r/sqrt(rho*c*pi*r^2);
a2=Q/(2*rho*c*r);
a3=3*Q/(4*sqrt(pi)*rho*c*r)*sqrt(1/(rho*c*r^2));

a1
a2
a3

tcf=zeros(N-1-start,1);
Tcf=zeros(N-1-start,1);

for i=1:1:N-1-start
    tcf(i,1)=t(i+start);
    Tcf(i,1)=Tep(i+start);
end

myfun=inline('0.3703*1/sqrt(beta(1))*tcf.^(-1/2)-
0.3226+0.2684*(beta(1))^(3/2)*tcf.^(1/2)',...
'beta','tcf');

beta=nlinfit(tcf,Tcf,myfun,1);
kcalc=beta(1);

kcalc

```

## **Vita**

Benjamin M. Rosenzweig was born on December 15<sup>th</sup>, 1988 in Morristown, New Jersey, the son of Donna and Alan Rosenzweig. After finishing high school at Parsippany Hills High School in 2007, he entered Lehigh University to study in the field of mechanical engineering and mechanics. He completed the Bachelor of Science degree in Mechanical Engineering and Mechanics in 2011. After completing his Bachelor of Science degree, he continued to pursue his Master of Science degree in Mechanical Engineering and Mechanics at Lehigh University, with which he graduated in 2012.